RAPID COMMUNICATIONS

PHYSICAL REVIEW E **75**, 020601(R) (2007)

Effect of stress on the diffusion-controlled dissolution of a spherical particle

Jérôme Colin*

Laboratoire de Métallurgie Physique, UMR 6630 du CNRS, Université de Poitiers, BP 30179, 86962 Futuroscope Cedex, France

(Received 22 September 2006; published 13 February 2007)

The diffusion-controlled dissolution of a spherical particle consisting in two epitaxially stressed solid phases of a substitutional binary alloy in contact with an undersaturated solution is investigated. A linear stability analysis of the solid-liquid interface demonstrates that a morphological instability of the particle may occur due to the epitaxial stress generated by the spherical precipitate embedded in the solid matrix, the liquid pressure being neglected. The critical radius of the particle below which the interface is unstable is determined and the conditions for the roughness development are discussed.

DOI: 10.1103/PhysRevE.75.020601 PACS number(s): 68.08.−p, 62.20.Dc, 68.35.Ct

In terms of solute diffusion, the morphological change of a growing spherical crystal has been first studied to the author's knowledge by Mullins and Sekerka [1]. These authors demonstrated that the gradient of concentration in a supersaturated solution is the driving force of the instability while the isotropic interfacial free energy has a stabilizing effect. The effect of interface kinetics and the conditions for self-similar evolution leading to shape invariant growing crystal have been also investigated [2–4]. The morphological change of a nonhydrostatically stressed planar solid has been first investigated in the linear regime by Asaro and Tiller [5], Grinfeld [6], and others [7,8]. For a growing spherical precipitate embedded in an infinite-size solid matrix, the epitaxial stress has been found to enhance the instability of the interface when the matrix is harder than the precipitate [9]. The destabilizing effect of composition stress on the morphology of a spherical particle growing in a supersatured solution has also been characterized [10].

Dissolution phenomena such as dissolution of salt in aqueous solution, dissolution of rock formations or second phase precipitate in metals have been widely investigated. The dissolution of a spherical particle in an undersaturated solution has already been described [1]. It has been emphasized that both effects of concentration gradient and interfacial free energy add to smooth the crystal shape. Recently, the study of the diffusion-limited dissolution of a 2D corrugated crystal has confirmed the decay of the initial grooves of the surface [11]. The study of the dissolution of a square cylinder using lattice-Boltzman's method has also shown that the front rounds [12]. The dynamics of a dissolution front for stressed planar salt crystals in contact with an aqueous fluid has been studied [13]. Both diffusion and dissolution are found to be limiting factors. Experimental studies [14,15] of the formation of alloys (Mo-Ni) by liquid phase sintering have been realized when other elements are added to the liquid or when heat treatment at a temperature different from that of the sintering is performed. The coherency strain appearing during the recrystallization of the new solid may induce interface instability. Recently, mechanofusion techniques have been developed [16] to produce two phases coated fine metallic particles where stress may also play an important role. In this paper, the critical effect of epitaxial stress on the interface morphology of a two-phase spherical particle in contact with an undersaturated solution is investigated.

A two component spherical solid is in contact with an isothermal undersaturated solution under pressure P_L. The solid is a substitutional binary alloy consisting in two phases epitaxially stressed through a coherent interface (see Fig. 1 for axes). The first solid phase is a spherical precipitate of radius R, shear modulus μ_p and Poisson's ratio ν embedded in a finite-size matrix of initial outer radius R_i, shear modulus μ_m and Poisson ratio's ν. In the following, both effects on the particle morphological change of interfacial stress and hydrostatic pressure P_L (in particular when $\mu_p \neq \mu_m$) are assumed to be much smaller than that of epitaxial stress and have not been considered. In the reference state [17], the matrix is stress free with its equilibrium lattice parameter while the precipitate in the matrix is stressed by $T_{ij}^{p,*} = -C_{ijkk}^{p}\epsilon^{p,*}$, with $\epsilon^{p,*}$ the eigenstrain located in the precipitate resulting from the misfit between the two phases [9], $T_{ij}^{p,*}$ the intrinsic stress in the precipitate and C_{ijkl}^{p} its elastic moduli. Linear isotropic elasticity theory is used and summation over repeated indices is implied. The atomic volumes of the two species are assumed to be of the same order of magnitude such that composition stress vanishes. Both solid and liquid are dilute solutions and the vacancies are neglected. The diffusion coefficient in the solid is taken to be zero. The concentration of the solute is fixed to C_S in the matrix. The position dependent concentration of the solute in the liquid is

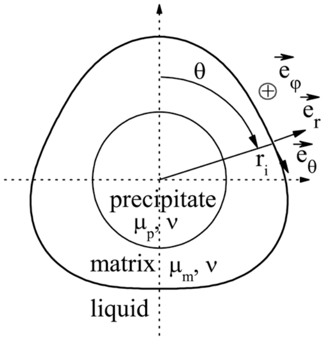

FIG. 1. The solid-liquid interface of a two phase spherical particle is perturbed with the help of the Y_3^0 harmonic (the scale is enlarged).

---

*Electronic address: jerome.colin@univ-poitiers.fr labeled $c_L(\vec{r})$, its uniform value at infinity is labeled c_L^{∞}. The equilibrium concentration of solute in the liquid at a flat interface under constant pressure is denoted by c_L^0 and at the general stressed interface by c_L^i. The study of the diffusion-controlled dissolution process requires that contrary to the growth case, $(c_L^0-c_L^{\infty})/c_L^0 \geqslant 0$. In the quasistationary approximation [1] where $|(c_L^{\infty}-c_L^i)/(C_S-c_L^i)| \leqslant |(c_L^{\infty}-c_L^0)/(C_S-c_L^0)| \ll 1$, it is assumed that c_L satisfies Laplace's equation $\Delta c_L(\vec{r})=0$. The condition of solute conservation yields

$$(C_S-c_L^i)V_n = D\vec{\nabla}c_L \cdot \vec{n}, \tag{1}$$

with $V_n=\dot{\vec{r}}_i\cdot\vec{n}$ the normal velocity of the interface located at $\vec{r}_i$, $\dot{\vec{r}}_i=dr_i/dt$ with t the time, $\vec{n}$ the unit vector normal to the interface pointing into the liquid and D the solute diffusion coefficient in the liquid. At the solid-liquid interface, the concentration c_L must satisfy the modified Gibbs-Thomson equation [9,18,19],

$$c_L^i = c_L^0 + c_L^0\Gamma\left(\kappa + \frac{1}{2\gamma}S_{ijkl}^m T_{ij}^m T_{kl}^m\right), \tag{2}$$

with κ the interfacial curvature and γ the interfacial free energy per unit surface. Within linear isotropic elasticity theory, S_{ijkl}^m is the elastic compliance tensor and T_{ij}^m the stress tensor due to epitaxy in the matrix taken at the interface. The constant Γ is defined by $\Gamma=\frac{\gamma V_0'(1-c_L^0)}{RT(c_S^0-c_L^0)}$ with V_0' the molar volume of lattice points in the reference state, c_S^0 the solute concentration in the matrix at a flat interface under constant pressure, R the gas constant, T the absolute temperature. The total displacement field $\vec{u}^k$ in the solid must satisfy Navier's equation [20],

$$\Delta\vec{u}^k + \frac{1}{1-2\nu}\vec{\nabla}(\operatorname{div}\vec{u}^k) = 2\frac{1+\nu}{1-2\nu}\vec{\nabla}\epsilon^{k,*}, \tag{3}$$

with $k=p,m$ and $\epsilon^{m,*}=0$. At the coherent precipitate-matrix interface, the mechanical equilibrium and the continuity of displacement read

$$(T_{ij}^p - T_{ij}^m)n_j^p = 0, \quad \vec{u}^p = \vec{u}^m, \tag{4}$$

with $\vec{n}^p$ the normal to the solid-solid interface pointing into the matrix. The traction free condition on the external surface of the particle at $\vec{r}_i$ requires that

$$T_{ij}^m n_j = 0. \tag{5}$$

The solid-liquid interface is perturbed with the help of the complete spherical harmonic Y_l^m such that $r_i=R_i+\epsilon A(R_i)Y_l^m(\theta,\varphi)$ with ϵ the dimensionless expansion parameter and $A(R_i)$ the amplitude of the interface fluctuation. The diffusion and elastic problems have been solved to the first order in ϵ parameter assuming that the quasistatic approximation holds and that the mechanical equilibrium is satisfied at all times in the solid. The elastic displacement and stress are developed as

$$\vec{u}^k = \vec{u}^{k,(0)} + \epsilon\vec{u}^{k,(1)} + \Theta(\epsilon^2), \tag{6}$$

$$T_{ij}^k = T_{ij}^{k,(0)} + \epsilon T_{ij}^{k,(1)} + \Theta(\epsilon^2), \tag{7}$$

with $k=p,m$. The general expression of the initial displacement field $\vec{u}^{k,(0)}$ satisfying the Eq. (3) is given by $\vec{u}^{k,(0)}(\vec{r}) = u_r^{k,(0)}(r)\vec{e}_r$ with $\vec{e}_r$ the unit radial vector and [20]

$$u_r^{k,(0)}(r) = A_k^0 r + \frac{B_k^0}{r^2} + \frac{1+\nu}{1-\nu}\frac{1}{r^2}\int_{r_*^k}^{r}\epsilon^{k,*}(r')r'^2dr', \tag{8}$$

with r_*^k a constant to be specified. One takes $r_*^p=0$ for the precipitate. Using linear elasticity, the strain tensor $E_{ij}^{k,(0)}$ is derived from this displacement field [20]. Using Hooke's law, the stress and strain tensors satisfy to $E_{ij}^{k,(0)}=S_{ijlm}^k(T_{lm}^{k,(0)}-T_{lm}^{k,*})$. Following Leo *et al.* [9,17], the displacement field $\vec{u}^{k,(1)}$ is written as

$$u_r^{k,(1)}(\vec{r}) = f_k(r)Y_l^m(\theta,\varphi), \tag{9}$$

$$u_\theta^{k,(1)}(\vec{r}) = g_k(r)\frac{\partial Y_l^m}{\partial\theta}(\theta,\varphi), \tag{10}$$

$$u_\varphi^{k,(1)}(\vec{r}) = g_k(r)\frac{1}{\sin\theta}\frac{\partial Y_l^m}{\partial\varphi}(\theta,\varphi), \tag{11}$$

with the functions f_k and g_k given by

$$f_k(r) = A_k^1 r^{l-1} + B_k^1 r^{l+1} + C_k^1 r^{-l-2} + D_k^1 r^{-l}, \tag{12}$$

$$g_k(r) = A_k^1\frac{r^{l-1}}{l} + \zeta B_k^1 r^{l+1} - C_k^1\frac{r^{-l-2}}{l+1} + \varsigma D_k^1 r^{-l}. \tag{13}$$

The coefficients ζ and ς are defined as follows:

$$\zeta = \frac{l+5-4\nu}{(l+1)(l-2+4\nu)}, \quad \varsigma = \frac{4-l-4\nu}{l(l+3-4\nu)}. \tag{14}$$

The resulting strain and stress tensors are also derived within linear elasticity theory. The general expression of the solute concentration in the fluid satisfying Laplace's equation is

$$c_L(\vec{r}) = c_L^{\infty} + \frac{E_L^0}{r} + \frac{F_L^1}{r^{l+1}}\epsilon A(R_i)Y_l^m(\theta,\varphi) + \Theta(\epsilon^2). \tag{15}$$

The different constants $A_k^0, B_k^0, A_k^1, B_k^1, C_k^1, D_k^1, E_L^0, F_L^1$ have been determined by expanding Eqs. (2), (4), and (5) to the first order in ϵ but are not explicitly given. Using Eq. (1), the time evolution equations of the radius of the interface R_i and of the perturbation amplitude $A(R_i)$ are finally found to be for $R_i \geqslant R$,

$$\frac{1}{R_i}\frac{dR_i}{dt} = -\tau(R_i)\left[1 + \frac{R_*}{R_i}(1+G_0^{\text{elas}})\right], \tag{16}$$

$$\frac{1}{A(R_i)}\frac{dA(R_i)}{dt} = -\tau(R_i)(l-1) \times \left[1 + \frac{R_*}{R_i}\left(\frac{(l+1)(l+2)}{2} + 1 + G_1^{\text{elas}}\right)\right], \tag{17}$$

with $\tau(R_i)=D(c_L^0-c_L^\infty)/[(C_S-c_L^{i,\text{sph}})R_i^2]\geqslant 0$, $c_L^{i,\text{sph}}=c_L^0[1+2\Gamma(1+G_0^{\text{elas}})/R_i]$ and $R_*=2\Gamma c_L^0/(c_L^0-c_L^\infty)$ [1]. The elasticity term G_0^{elas} is given by

$$G_0^{\text{elas}}=\frac{9\mu_p^2(1-\nu)^2}{16(1+\nu)(1-2\nu)^2}\frac{R^6}{R_{\text{ATG}}R_i^5}\times\frac{1}{\left[\mu_m\left(1-\frac{R^3}{R_i^3}\right)+\mu_p\left(\frac{1+\nu}{2(1-2\nu)}+\frac{R^3}{R_i^3}\right)\right]^2},\qquad(18)$$

with $R_{\text{ATG}}=\mu_m\gamma/[(1-\nu)T_0^2]$ the Asaro-Tiller-Grinfeld radius and the stress $T_0=2\mu_m\epsilon^{p,*}(1+\nu)/(1-\nu)$. The elasticity term G_1^{elas} which is a nontrivial function of μ_p, μ_m, R, and R_i is not explicitly given here. In the case where $\mu_m=\mu_p$ and for $l\geqslant 2$, it simplifies as

$$G_1^{\text{elas}}=-\frac{R^6}{R_{\text{ATG}}R_i^5}\frac{f(l,\nu)}{g(l,\nu)},\qquad(19)$$

with

$$f(l,\nu)=7(1+\nu)+l\{19+20\nu+2l[11+l(l+5)]+l[20+l(11+2l)]\nu\},\qquad(20)$$

$$g(l,\nu)=4(l-1)(1+\nu)[l^2+(1+2\nu)l+1+\nu].\qquad(21)$$

From Eqs. (16) and (18), it can be observed that the dissolution of the spherical particle is affected by elasticity since the dissolution rate $|dR_i/dt|$ is increased by the positive term G_0^{elas}. From Eqs. (17) and (19)–(21), it is found that the terms in the growth rate of the fluctuation $dA(R_i)/dt$ due to the interfacial free energy and concentration gradient are negative and thus favor the decay of the harmonic. The elasticity term $-G_1^{\text{elas}}$ is always positive and favors its growth. This behavior is persistent in the general case where $\mu_p\neq\mu_m$. As a consequence, the elasticity contribution to the time evolution Eq. (17) of the harmonic is stated to be the only source of destabilization of the solid-liquid interface. In the case of growth, when the solution is supersaturated, i.e., when $c_L^\infty-c_L^0\geqslant 0$, the concentration gradient is the main source of interface destabilization [1]. The elasticity term calculated here is also assumed to participate to the morphological change but its effect is suspected to be limited since G_1^{elas} decreases as the particle grows. As a consequence, one may have $G_1^{\text{elas}}\leqslant 1+(l+1)(l+2)/2$ for sufficiently high values of R_i. The translation ($l=1$) mode is not considered [10] and the morphological change is investigated when at least the second harmonic Y_2^m develops. The critical radii $R_i^c(l=2)$ and $R_i^c(l=3)$ below which $(1/A)(dA/dt)\geqslant 0$ and the second and third harmonics Y_2^m and Y_3^m may appear are plotted in Fig. 2 as a function of R_{ATG}/R_* for $R=20R_*$, $\mu_p/\mu_m=1.5$, and $\nu=0.343$. It can be observed that as R_{ATG} decreases, the critical radii increase demonstrating thus that the higher the intrinsic stress is the sooner the morphological change appears

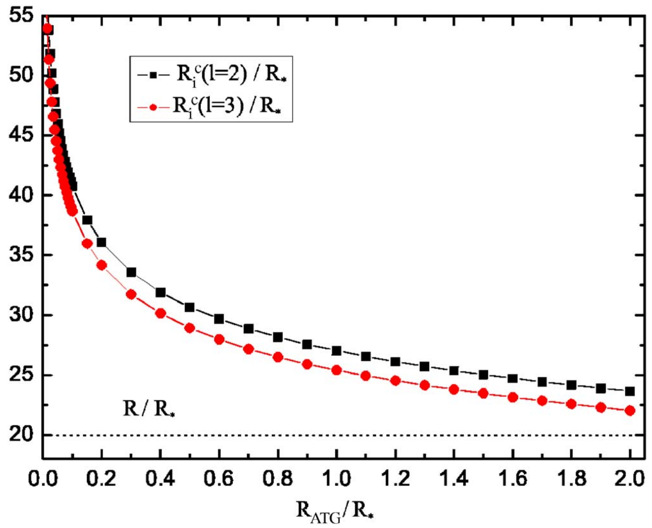

FIG. 2. (Color online) $R_i^c(l=2)/R_*$ and $R_i^c(l=3)/R_*$ versus R_{ATG}/R_* for $\mu_p/\mu_m=1.5$ and $R=20R_*$.

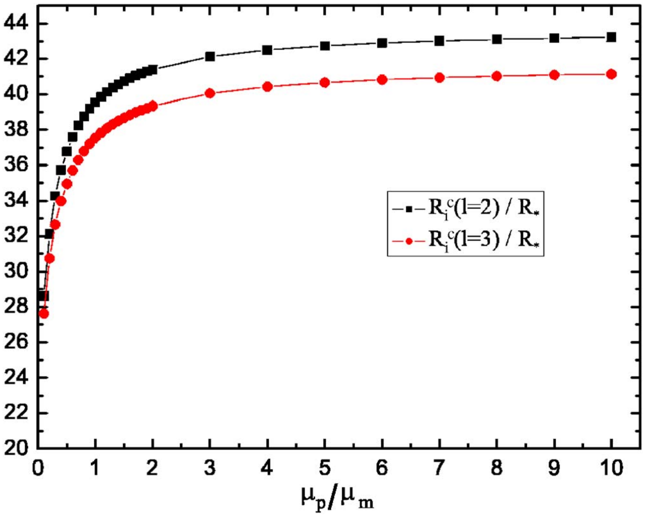

FIG. 3. (Color online) $R_i^c(l=2)/R_*$ and $R_i^c(l=3)/R_*$ versus μ_p/μ_m for $R_{\text{ATG}}/R_*=0.1$ and $R=20R_*$.

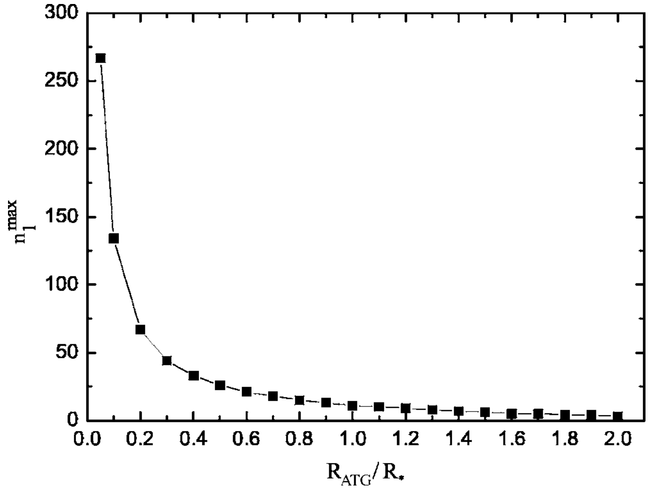

FIG. 4. The maximum number of harmonics with $l\geqslant 2$ susceptible to appear versus R_{ATG}/R_* for $\mu_p/\mu_m=1.5$, $R_i\rightarrow R$ and $R=20R_*$.

during the dissolution process. For a copper-based alloy, taking $R=8.314\ \mathrm{J\ mol^{-1}\ K^{-1}}$, $T=400\mathrm{K}$, $V_0'=7.12\ \mathrm{cm^3\ mol^{-1}}$, $\gamma=1.4\ \mathrm{J\ m^{-2}}$, $c_L^0=0.01$, $(c_L^0-c_L^\infty)/c_L^0=0.1$, $c_S^0=0.1$, $\mu_m=48\ \mathrm{GPa}$, and $\epsilon^{p,*}=0.6\%$, one gets the following order of magnitude for the physical parameters of the problem $R_{\mathrm{ATG}}/R_*=0.1$. In Fig. 3, the critical radii $R_i^c(l=2)$ and $R_i^c(l=3)$ are then plotted as a function of the ratio of shear moduli μ_p/μ_m for $R=20R_*$ and $R_{\mathrm{ATG}}=0.1R_*$. It can be observed that the morphological change is enhanced when the precipitate becomes harder, i.e., when $\mu_p/\mu_m>1$, and the initial elastic energy density resulting from epitaxy increases at the solid-liquid interface. In Fig. 4, the maximum theoretical number of harmonics $n_l^{\max}$ (with $l\geqslant 2$) susceptible to appear on the interface before the complete dissolution is achieved, i.e., when $R_i\rightarrow R$, is finally plotted versus R_{ATG}/R_* for $\mu_p/\mu_m=1.5$. It is found that for $R_{\mathrm{ATG}}/R_*=0.1$, $n_l^{\max}$ may be of the order of 100. Providing thus that the dissolution is not too fast and the epitaxy is sufficiently high, several harmonics may interact in the nonlinear regime of evolution leading to a rough interface. It is concluded that even though the elastic effect must overcome the conjugate stabilizing effects of the concentration gradient and interfacial energy, the development of the roughness due to epitaxial stress on a finite time scale corresponding to a partial dissolution of the solid matrix may be important.

In this paper, the linear analysis of the kinetics of the solid-liquid interface of a spherical particle in contact with an undersaturated solution has demonstrated that the epitaxial stress is at the origin of the morphological change of the crystal. It can finally be emphasized that the present analysis may have applications in other fields than metallurgy. It would be, for example, relevant to investigate the stress effect on the functional degradation of biodegradable implants or on the dissolution of geomaterials of various geometries in contact with aqueous solutions [12].

---

[1] W. W. Mullins and R. F. Sekerka, J. Appl. Phys. **34**, 323 (1963).

[2] S. R. Coriell and R. L. Parker, *Crystal Growth*, edited by H. S. Peiser (Pergamon, Oxford, 1967), p. 703.

[3] V. Cristini and J. Lowengrub, J. Cryst. Growth **240**, 267 (2000).

[4] V. Cristini and J. Lowengrub, J. Cryst. Growth **552**, 266 (2004).

[5] R. J. Asaro and W. A. Tiller, Metall. Trans. **3**, 1789 (1972).

[6] M. A. Grinfeld, Dokl. Akad. Nauk SSSR **290**, 1358 (1986).

[7] B. J. Spencer, P. W. Voorhees, and S. H. Davis, Phys. Rev. Lett. **67**, 3696 (1991).

[8] D. J. Srolovitz, Acta Metall. **37**, 621 (1989).

[9] P. H. Leo and R. F. Sekerka, Acta Metall. **37**, 3139 (1989).

[10] B. Caroli, C. Caroli, B. Roulet, and P. W. Voorhees, Acta Metall. **37**, 257 (1989).

[11] M. Z. Bazant, Phys. Rev. E **73**, 060601(R) (2006).

[12] F. Verhaeghe, S. Arnout, B. Blanpain, and P. Wollants, Phys. Rev. E **73**, 036316 (2006).

[13] C. Misbah, F. Renard, and J. P. Gratier, Geophys. Res. Lett. **31**, L06618 (2004).

[14] W. H. Rhee and D. N. Yoon, Acta Metall. **35**, 1447 (1987).

[15] W. H. Rhee and D. N. Yoon, Acta Metall. **37**, 221 (1989).

[16] J. Stein, M. Tenhover, and T. Toyakazu, Dtsch. Krankenpflegez **79**, 11 (2004).

[17] P. H. Leo, J. Iwan, J. I. D. Alexander, and R. Sekerka, Acta Metall. **33**, 985 (1985).

[18] F. C. Larché and J. W. Cahn, Acta Metall. **33**, 331 (1985).

[19] J. I. D. Alexander and W. C. Johnson, J. Appl. Phys. **58**, 816 (1985).

[20] B. A. Boley and J. H. Weiner, *Theory of Thermal Stresses* (Wiley, New York, 1960).